Geophys. J. Int. (2009) **179,** 1232–1244 doi: 10.1111/j.1365-246X.2009.04358.x

Required source distribution for interferometry of waves and diffusive fields

Yuanzhong Fan and Roel Snieder

Department of Geophysics and Center for Wave Phenomena, Colorado School of Mines, Golden, CO 80401, *USA. E-mail: yfan@mines.edu*

Accepted 2009 August 10. Received 2009 August 10; in original form 2008 September 24

SUMMARY

The Green's function that describes wave propagation between two receivers can be reconstructed by cross-correlation provided that the receivers are surrounded by sources on a closed surface. This technique is referred to as 'interferometry' in exploration seismology. The same technique for Green's function extraction can be applied to the solution of the diffusion equation if there are sources throughout in the volume. In practice, we have only a finite number of active sources. The issues of the required source distribution is investigated, as is the feasibility of reconstructing the Green's function of the diffusion equation using a limited number of sources within a finite volume. We study these questions for homogeneous and heterogeneous media for wave propagation and homogeneous media for diffusion using numerical simulations. These simulations show that for the used model, the angular distribution of sources is critical in wave problems in homogeneous media. In heterogeneous media, the position and size of the heterogeneous area with respect to the sources determine the required source distribution. For diffusion, the sensitivity to the sources decays from the midpoint between the two receivers. The required width of the source distribution decreases with frequency, with the result that the required source distribution for early- and late-time reconstruction is different. The derived source distribution criterion for diffusion suggests that the cross-correlation-based interferometry is difficult to apply in field condition.

Key words: Interferometry; Controlled source seismology; Wave scattering and diffraction.

1 INTRODUCTION

The term interferometry generally refers to the study of the interference of two signals as a measure of the difference between them (Curtis *et al.* 2006). The term also refers to the technique used in seismology to extract the response which describes the wave propagating between two receivers, as if one of the receivers were an active source (Lobkis & Weaver 2001; Derode *et al.* 2003; Snieder 2004, 2007; Wapenaar 2004; Weaver & Lobkis 2004; Wapenaar *et al.* 2005). This technique has been applied in ultrasound (Weaver & Lobkis 2001; Malcolm *et al.* 2004; Larose *et al.* 2006; van Wijk 2006), crustal seismology (Campillo & Paul 2003; Roux *et al.* 2005; Sabra *et al.* 2005a,b; Shapiro *et al.* 2005), exploration seismology (Bakulin & Calvert 2004; Calvert *et al.* 2004; Bakulin & Calvert 2006; Mehta & Snieder 2008), helioseismology (Rickett & Claerbout 1999), structural engineering (Snieder & Şafak 2006; Snieder *et al.* 2006) and numerical modelling (van Manen *et al.* 2005). Seismic interferometry was first applied to wave propagation in non-attenuating and time-reversal invariant media (Lobkis & Weaver 2001; Derode *et al.* 2003; Snieder 2004; Wapenaar 2004; Weaver & Lobkis 2004). Later, it was shown that interferometry can not only be applied to wavefields, but also to diffusive fields (Snieder 2006b). Recent proofs have been given showing that the Green's function can be extracted for a wide class of linear systems including those that are attenuating, as well as those that may not be invariant for time-reversal because of flow (Godin 2006; Wapenaar 2006b; Wapenaar *et al.* 2006; Snieder *et al.* 2007; Weaver 2008).

Seismic interferometry in the exploration geophysics community is also referred to as the 'virtual source method' (Bakulin & Calvert 2004, 2006; Calvert *et al.* 2004), and has been applied to imaging (Mehta *et al.* 2007; Vasconcelos *et al.* 2007). The sources used in seismic interferometry can be either controlled shots (Bakulin & Calvert 2004, 2006; Calvert *et al.* 2004; Schuster *et al.* 2004; van Wijk 2006; Mehta *et al.* 2007) or ambient noise (Roux *et al.* 2005; Shapiro *et al.* 2005; Weaver 2005; Curtis *et al.* 2006; Godin 2006; Stehly *et al.* 2006; Miyazawa *et al.* 2008).

Although the extraction of the Green's function is usually based on cross-correlation, deconvolution can also be used (Snieder & Şafak 2006; Vasconcelos & Snieder 2008a,b). The term 'interferometry' in this paper refers to cross-correlation based interferometry. Interferometry applied to acoustic waves can be expressed in the frequency domain as (Snieder *et al.* 2007)

$$G(\mathbf{r}_A, \mathbf{r}_B, \omega) - G^*(\mathbf{r}_A, \mathbf{r}_B, \omega) = \oint_S \frac{1}{\rho}\{G^*(\mathbf{r}_A, \mathbf{r}, \omega)\nabla G(\mathbf{r}_B, \mathbf{r}, \omega) - [\nabla G^*(\mathbf{r}_A, \mathbf{r}, \omega))G(\mathbf{r}_B, \mathbf{r})]\widehat{\mathbf{n}} \cdot \mathrm{d}S, \quad (1)$$

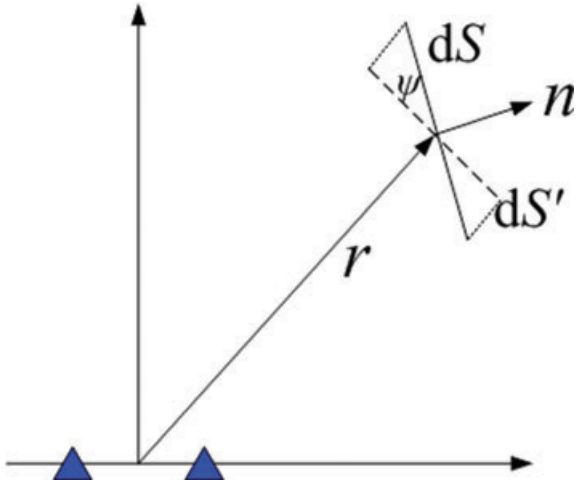

Figure 1. An arbitrary surface element dS and its projection dS'.

where $G(\mathbf{r}_A, \mathbf{r}_B, \omega)$ is the pressure Green's function that describes wave propagation from $\mathbf{r}_B$ to $\mathbf{r}_A$, respectively, $*$ indicates complex conjugation, S is the surface where sources are located, $\hat{\mathbf{n}}$ is the unit vector perpendicular to the surface dS, ω the angular frequency, ρ the density and c the wave velocity. When the waves satisfy a radiation boundary condition on the surface S, $\nabla G(\mathbf{r}_A, \mathbf{r}, \omega) \approx \mathrm{i}(\omega/c)G(\mathbf{r}_A, \mathbf{r}, \omega)\hat{\mathbf{r}}$, and eq. (1) becomes

$$G(\mathbf{r}_A, \mathbf{r}_B, \omega) - G^*(\mathbf{r}_A, \mathbf{r}_B, \omega) \approx 2\mathrm{i}\omega \oint_S \frac{1}{\rho c} G(\mathbf{r}_A, \mathbf{r}, \omega) G^*(\mathbf{r}_B, \mathbf{r}, \omega)(\hat{\mathbf{r}} \cdot \hat{\mathbf{n}})\mathrm{d}S. \quad (2)$$

Thus, the integration over all source positions of the cross-correlation of $G(\mathbf{r}_A, \mathbf{r}, \omega)$ and $G(\mathbf{r}_B, \mathbf{r}, \omega)$ yields the superposition of the causal Green's function $G(\mathbf{r}_A, \mathbf{r}_B, \omega)$ and time-reversed Green's function $G^*(\mathbf{r}_B, \mathbf{r}, \omega)$. Using the geometric relationship defined in Fig. 1, eq. (2) becomes

$$G(\mathbf{r}_A, \mathbf{r}_B, \omega) - G^*(\mathbf{r}_A, \mathbf{r}_B, \omega) \approx 2\mathrm{i}\omega \oint_{S'} \frac{1}{\rho c} G(\mathbf{r}_A, \mathbf{r}, \omega) G^*(\mathbf{r}_B, \mathbf{r}, \omega)\mathrm{d}S', \quad (3)$$

in which $\mathrm{d}S' = \mathrm{d}S \cos\psi$ is the projection of the surface element dS on a circle with radius r. A similar mathematical expression exists for the extraction of the Green's function for diffusion. The main difference is that the surface integral becomes a volume integral (Snieder 2006b)

$$G(\mathbf{r}_A, \mathbf{r}_B, \omega) - G^*(\mathbf{r}_A, \mathbf{r}_B, \omega) = 2\mathrm{i}\omega \int_V G(\mathbf{r}_A, \mathbf{r}, \omega) G^*(\mathbf{r}_B, \mathbf{r}, \omega)\mathrm{d}V, \quad (4)$$

in which V is the volume containing the sources. The meaning of other terms are the same as those in eq. (3).

Eqs (3) and (4) show that the main difference between wave equation and diffusion equation interferometry is the required source distribution. For waves, eq. (3) shows that if two receivers are surrounded by active sources on a closed surface, the response that describes waves propagating between two receivers can be reconstructed as if one of the receivers were an active source. For diffusion, eq. (4) states that sources are required to be everywhere in the volume (Snieder 2006b). In practice, there are only a finite number of sources. Therefore, we can never have a closed source surface for waves or sources throughout the volume for diffusion. This raises the question: what is the required source density and how should we locate these sources in order to reconstruct the Green's function accurately?

The importance of cross-correlation-based interferometry for waves has been addressed by numerous authors. Cross-correlation-based interferometry for diffusion is still at the theory stage. In exploration geophysics, there are at least two important diffusive fields: pore pressure and low-frequency inductive electromagnetic fields. From the pore pressure we can infer the fluid conductivity between wells (Bourdet 2002; Kutasov *et al.* 2008). Electromagnetic fields carry information about the resistivity of the pore fluid and may thus help distinguish between hydrocarbons and water. For offshore oil exploration, controlled-source electromagnetic (CSEM) is an important technique used to detect hydrocarbons (Hoversten *et al.* 2006; Constable & Srnka 2007; Darnet *et al.* 2007; Scholl & Edwards 2007).

2 MODEL AND RESULTS

We study the required source distribution in both homogeneous and heterogeneous media for waves, and a homogeneous model for diffusion, with a finite number of sources using numerical experiments. In the next section, we discuss these simulations, providing explanations of the observations. We first show numerical experiments demonstrating the extraction of wave equation Green's function.

2.1 Waves in homogeneous media

For simplicity we first show numerical tests using a 2-D model with a velocity of 1 km s^{-1}. To define the source position, we use two parameters: the source angle and source radius as shown in Fig. 2. A and B are two receivers with a separation b. The vectors connecting the source to the two receivers are denoted by $\mathbf{r}_{SA}$ and $\mathbf{r}_{SB}$, respectively. The source function we use for the examples in the wave part for homogeneous media is a Ricker wavelet with a central frequency of 0.5 Hz. The source amplitude is the same for all sources in all the experiments in this paper.

2.1.1 Experiment 1: uniformly distributed source angle

We first study the effect of the source angle distribution. Sources are uniformly distributed on a circle with a radius of 40 km. The distance

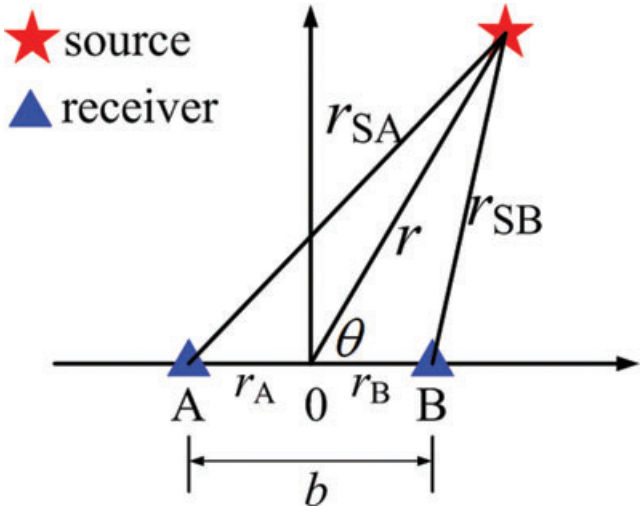

Figure 2. Definition of the source radius r and source angle θ that define a source position in 2-D.

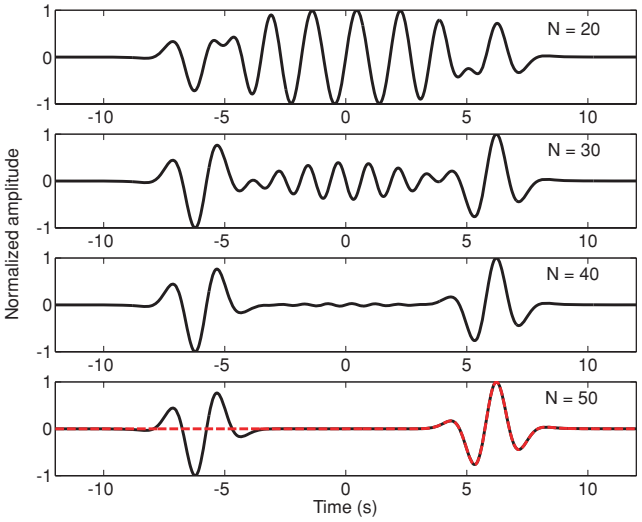

Figure 3. Reconstructed responses (solid lines) for uniform angle distribution with different number of source N (the dashed line in the bottom panel is the exact response between the two receivers).

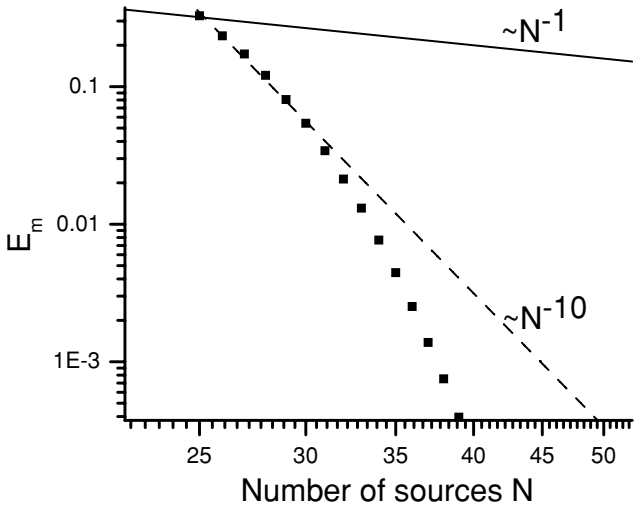

Figure 4. Fluctuation energy decay as a function of number of sources N for the uniform angular distribution of sources. The dashed and solid line represent two different power laws in the log–log coordinate system.

between the two receivers is 6 km. Fig. 3 shows the reconstructed response between the two receivers for a homogeneous distribution of sources with increasing number of sources. The response has two parts, the causal and anticausal parts as represented by eq. (3). The causal part of the signal represents the signal propagating from receiver A to B and the anticausal part is the time-reversal of this, that is, the signal propagating from receiver B to A. If we replace one of the receivers with an active source, the received signal arrives after a propagation time of 6 s. To make the shape of the received signal the same as that of the reconstructed signal, we correlate the received signal with the source-time function. This new signal is represented by the dashed line in the bottom panel and is virtually indistinguishable from the causal part of the reconstructed response with 50 sources (the amplitudes of both reconstructed and active signals are normalized). The main point in Fig. 3 is that the oscillations observed in the middle part of the reconstructed signal decreases with increasing number of sources N. Hence, a minimum source density needs to be exceeded for extracting the response successfully. This required source density is derived in the discussion part of this section.

We quantify the spurious fluctuations that arrive between the anticausal and the causal response by defining the fluctuation energy

$$E_m = \frac{1}{N_m} \sum_{i=1}^{N_m} A[i]^2, \tag{5}$$

in which N_m is the number of the discrete sample points in the middle part of the signal (i.e. the part between the two main pulses), $A[i]$ is the amplitude of the ith sample point in the middle part. Fig. 4 shows this fluctuation energy decay as a function of number of sources N. Weaver & Lobkis (2005) showed that these fluctuations decay as N^{-1} if the sources are randomly distributed. Fig. 4 shows that when the sources are uniformly distributed in angle, the decay rate is much faster than N^{-1}. The reason of this is shown in the discussion part of the wave problem.

Note that the sources are always distributed starting from angle zero (the line crossing two receivers) in the example. By doing this, there is always a source located at angle zero (one stationary point). If the starting point of angle distribution is arbitrary, the energy fluctuation behaviour with a small number of sources is

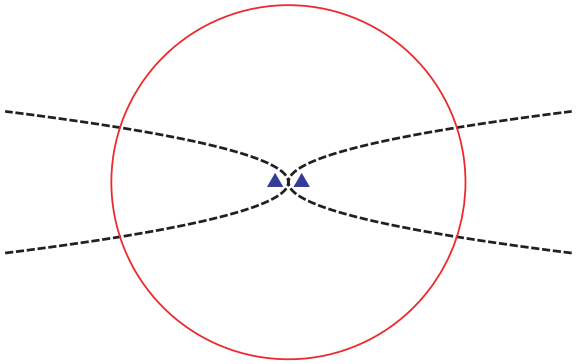

Figure 5. Stationary phase zone (denoted by the dashed curves) in a homogeneous medium.

not exactly the same as the one shown in Fig. 4. This difference in the energy fluctuation is caused by different sampling of the stationary phase zone by sources. The stationary phase zones for the configuration in this example are shown by the dashed curves in Fig. 5. The sources that are located in the stationary phase zones give the most contribution to the physical arrivals in the Green's function reconstruction (Snieder 2004). For small number of sources, the sampling of the stationary phase zone is sensitive to where the first source is located. Therefore, the decaying behaviour of the energy fluctuation E_m varies depending on where the first source is located when the number of sources is small ($<$50 in this case). With a large number of sources, it does not matter anymore where the first source is located because the stationary phase zone can always be sampled sufficiently.

2.1.2 Experiment 2: randomly distributed source angle

In this experiment, the source angles are randomly distributed with constant source radius. Fig. 6 shows the reconstructed response as a function of the number of sources N for a random angular distribution of sources along the circle. Compared with Fig. 3, the random distribution gives a much poorer reconstruction than does the uniform distribution with the same number of sources.

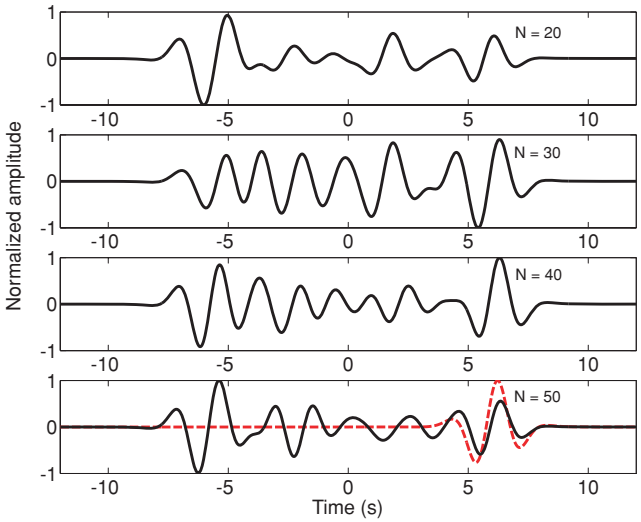

Figure 6. Reconstructed responses (solid lines) for random angular distribution with different number of sources N (the dashed line in the bottom panel is the exact response between the two receivers).

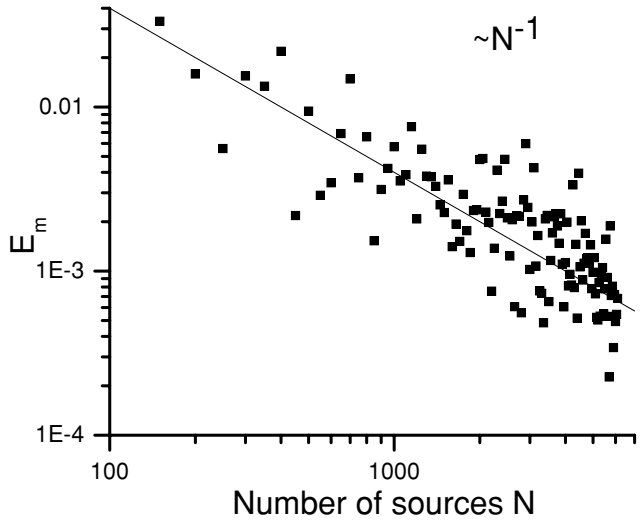

Figure 7. Fluctuation energy decay as a function of number of sources N for the random angular distribution of sources. The solid line represents a N^{-1} power-law decay in the log–log coordinate system.

Fig. 7 shows this fluctuation energy decay, as defined in eq. (5), as a function of N for randomly distributed sources. The fluctuation decay behaviour is consistent with the prediction of Weaver & Lobkis (2005): the decay is proportional to N^{-1}. In contrast to the uniform distribution, it does not matter where the first source is located for the random distribution. In this experiment, the source radius remains much larger than the distance between the two receivers. If the radius is very small (for example, 6 km), the fluctuation E_m decays more slowly ($N^{1/2}$) because the radiation boundary condition that reduces eqs (1) to (2) is inaccurate. Experiment 2 suggests that not only the number of sources is important, but also their angular distribution. The difference of this decay rate of uniformly and randomly distributed sources is explained in the discussion part of this section.

2.1.3 *Experiment 3: smooth source angle distribution*

From experiments 1 and 2, we might conclude that the source angle needs to be uniformly distributed with angle to apply this technique successfully with a small number of sources. Fig. 8 shows that the angles not necessary have to be uniformly distributed but may be smoothly varying. Next we show examples with non-uniform but smoothly varying angle distribution where the response is accurately reconstructed. In the example shown in Fig. 8, the sources are uniformly distributed on a circle with the centre of the two receivers moved away from the centre of the circle [from (0,0) to (−5,6)]. This makes the source angle distribution no longer uniform, but it's still smooth. The numerical simulation shows accurate reconstruction of the response from 50 sources. The amplitude differences of the causal and anti-causal parts are due to the different energies from the two stationary-phase zones on the left- and right-hand side of the receivers as illustrated by the two dashed curves in the upper panel of Fig. 8. Only sources within these two stationary zones contribute to the extraction of the direct wave (Snieder 2004; Roux *et al.* 2005). In this case, the stationary zone on the right-hand side corresponds to the causal pulse and the left-hand side stationary zone corresponds to the anticausal pulse. In the right-hand side stationary zone there are more sources than on the left-hand side. This explains why the causal pulse is stronger than the anticausal one. Note that the distance of the sources to the midpoint of the receiver locations is not constant in this experiment. In the example shown in Fig. 9, the sources are uniformly distributed on the sides of a triangle. The source angle is not uniform but is smoothly varying. The lower panel in Fig. 9 shows that for 72 sources, the reconstruction of the response is still accurate. In this case, the required number of sources is slightly larger than that for the uniform distribution but much smaller than for the accurate reconstruction of the Green's function with the random source distribution. The value of this number depends on the smoothness of the angular variation. Similar to an acquisition geometry with sources along a line (Bakulin & Calvert 2006; Mehta *et al.* 2007), the source radius now varies with the source position. Note that in this example the source radii are much larger than the distance between the two receivers. Thus, the influence of varying source radii is negligible. This is shown in detail in the next experiment.

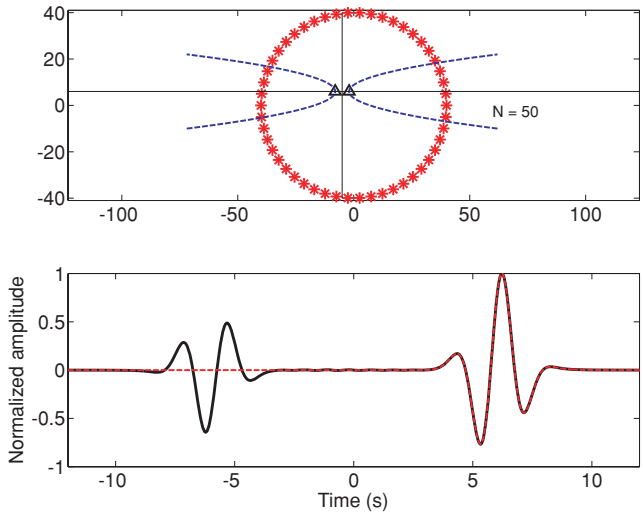

Figure 8. Reconstructed response (solid line in the lower panel, dashed line is the exact response) for a smoothly varying source angle distribution (upper panel).

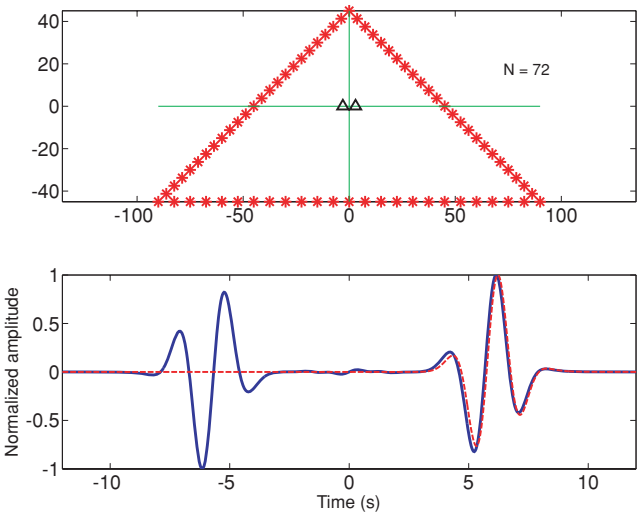

Figure 9. Reconstructed response (solid line in the lower panel, dashed line is the exact response) for source spaced equidistantly on a triangle (upper panel).

2.1.4 Experiment 4: varying source radius

In the previous three experiments we learned how the angular distribution influences the response extraction. The uniform angular distribution has a faster decay rate of the fluctuation energy $E_m\,(N^{-10})$ than for the random angular distribution (N^{-1}). The number of sources required for a smoothly varying angle distribution is between these two extreme cases and it depends on how smooth the angular distribution is. There is, however, still another parameter: the radius r as defined in Fig. 2. In this example we compare the result from two distributions with the same angular distribution but different source radii. The first one is the example we showed in experiment 1, when 50 sources are uniformly distributed on a circle (stars in the upper panel of Fig. 10). The second one is for sources with the same angle distribution but the radius is randomly varying in a range in which all radii are much larger than the distance between the two receivers (dots in the upper panel of Fig. 10. The reconstructed responses in Fig. 10 suggest that varying the source radii does not degrade the accuracy of the Green's function extraction. This is only true when source radii are much larger than the distance between the two receivers. The reason for this is explained in the discussion part.

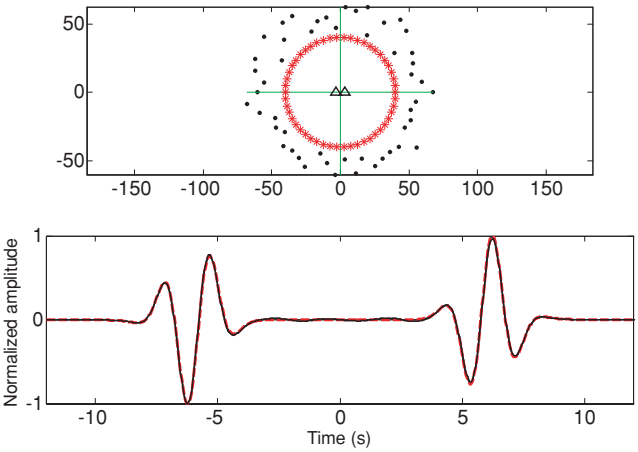

Figure 10. Two source distributions with the same angular distribution but different radii (top panel) and the reconstructed responses: solid (same radius), dashed line (different radius).

2.2 Waves in heterogeneous media

It is commonly believed that the source distribution is less important for the heterogeneous medium than for a homogeneous medium because the heterogeneity scatters the wave fields into different directions. In an extreme case, one might think that one source is sufficient to reconstruct the Green's function if the medium is sufficiently complicated. In this study, we find that these beliefs are not correct and more sources are required to reconstruct the full Green's function for a strongly heterogeneous medium than for an homogeneous medium.

The heterogeneous medium in this section consists of 200 isotropic point scatterers in a 80 m $\times$ 80 m square around the two receivers. The source radius is 90 m and the receivers are 20 m apart. The wavefield was modelled using the theory of Groenenboom & Snieder (1995), which takes all multiple scattering events into account. The waveform is a Gaussian wavelet with 600 Hz the centre frequency and bandwidth 400 Hz. The phase velocity in the background medium is 1500 m s^{-1}.

Fig. 11 shows the reconstructed responses between the two receivers using full illumination (sources uniformly distributed around the medium) and one single source. The red dashed curve is the signal received by one receiver when the other one acts as a real source. The black solid curve is the signal reconstructed by interferometry. Panel (a) shows the reconstruction when 300 uniformly distributed sources are used while panel (c) is the case when a single source is used. Panels (b) and (d) are the enlarged version of panels (a) and (c), respectively. The correlation coefficient between the exact and the causal part of the extracted signal is 0.97 for the 300 uniformly distributed sources while it is -0.03 for the single source. In this scattering medium, the wavefield from a single source is equipartitioned, see the discussion part. Perhaps surprisingly, the reconstructed signal from a single source does not represent the Green's function between the two receivers at all. We also find that more sources are needed to reconstruct the Green's

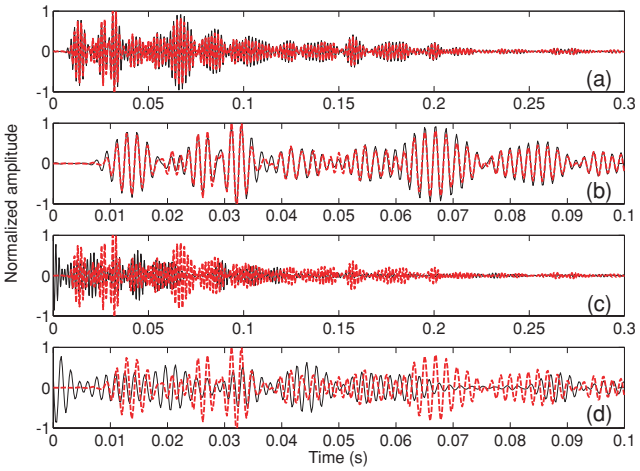

Figure 11. The Green's function reconstruction in a strongly scattering medium. The red dashed curve is the active experiment and the black solid curve is the reconstruction. Panel (a) shows the reconstruction when 300 uniformly distributed sources are used while panel (c) is the case when a single source is used. Panels (b) and (d) are the enlarged version of panels (a) and (c), respectively.

function accurately for this heterogeneous medium (300 sources) than for a homogeneous medium (140 sources) with the same velocity, source wavelet and source distribution. Derode *et al*. (2003) reached a similar observation based on their finite difference simulations. An explanation and required source density in an strongly scattering medium is given in the discussion section.

2.3 Diffusion

Eq. (4) shows that we need sources in the entire volume to extract the diffusion Green's function. To simplify the problem, we first analyse a 1-D medium with a constant diffusion coefficient and then extend our investigations to 3-D.

2.3.1 Experiment 1: diffusion Green's function recovery in 1-D

We choose the origin of the coordinate system to be the mid-point between the two receivers. The separation of the two receivers is 2 km. The diffusion coefficient used in this model is $D = 1\ \mathrm{km^2\ s^{-1}}$. We distribute sources uniformly on the 1-D line with the centre of the distribution at origin. Fig. 12 shows the geometry of 1-D source distribution. We define two parameters to characterize this source distribution. As shown in Fig. 12, W_s is the width of the distribution and $\rho_s = N/W_s$ is the source density. Next we test three different distributions. The first is a distribution with narrow width W_s and high source density ρ_s (Fig. 13). The second is a distribution with the same number of sources, but with a wide width W_s and low density (Fig. 14). The third distribution has more sources and has wide W_s and high density ρ_s (Fig. 15). Figs 13–15 show that different

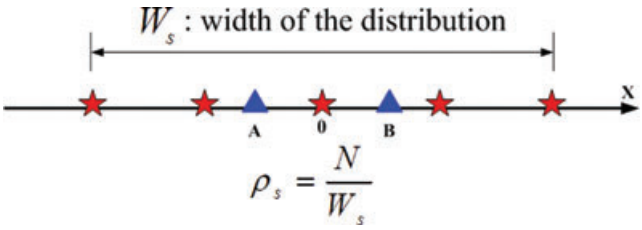

Figure 12. 1-D source distribution and the definitions of geometric parameters.

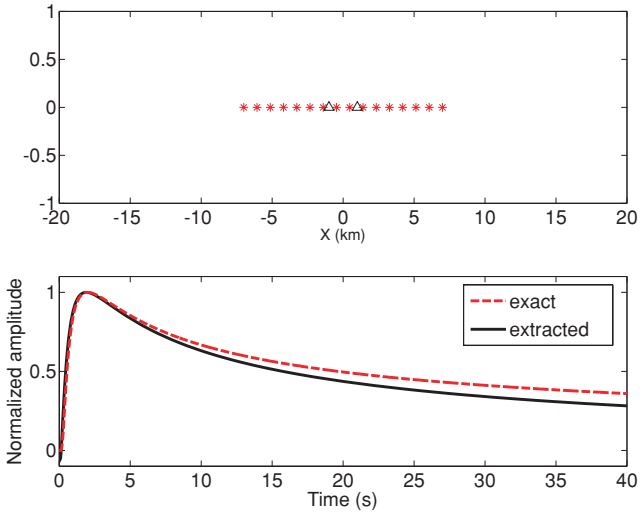

Figure 13. 1-D source distribution (upper panel) with $Ws = 14$ km, $\rho_s = 1.143\ \mathrm{km^{-1}}$ and the extracted Green's function (lower panel).

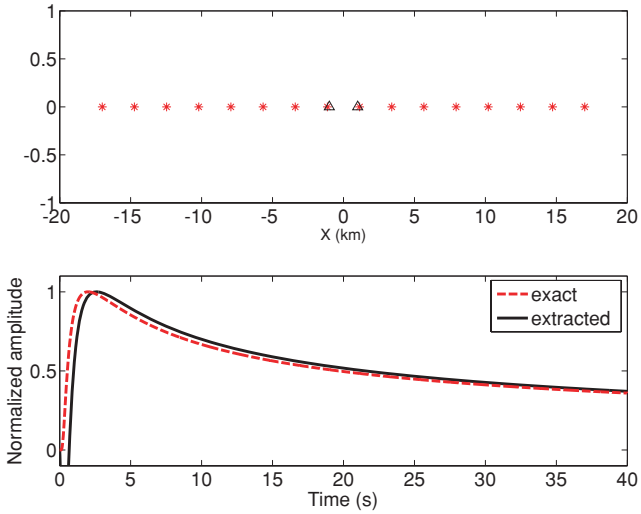

Figure 14. 1-D source distribution (upper panel) with $Ws = 34$ km, $\rho_s = 0.47\ \mathrm{km^{-1}}$ and the extracted Green's function (lower panel).

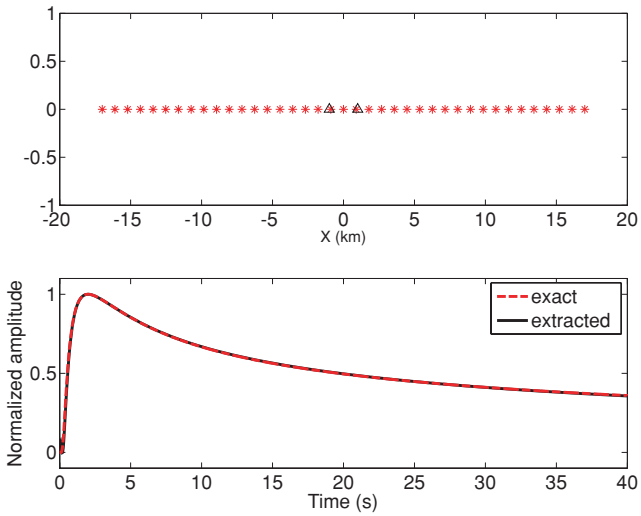

Figure 15. 1-D source distribution (upper panel) with $Ws = 34$ km, $\rho_s = 1.147\ \mathrm{km^{-1}}$ and the extracted Green's function (lower panel).

source distributions are needed for the accurate reconstruction of the early- and the late-time response. The early-time response is defined as the response before the peak in the Green's function of the diffusion equation, the late-time part is defined as the response after the main peak. The early-time reconstruction is controlled by the source density ρ_s (Figs 13 and 15) and late-time reconstruction is more affected by the distribution width Ws (Figs 14 and 15).

2.3.2 Experiment 2: Green's function reconstruction for diffusion in 3-D

Following the same strategy we extend the diffusion experiment to 3-D. Instead of putting the sources on a line, we uniformly distributed them in a cube. We define W_s as the side length of the cube, and the source density is defined as $\rho_s = N/(W_s)^3$.

In Fig. 16(a), a source distribution with small W_s is used. As in 1-D, the early-time of the Green's function is reconstructed well, but the late-time behaviour is not. When the width of the distribution

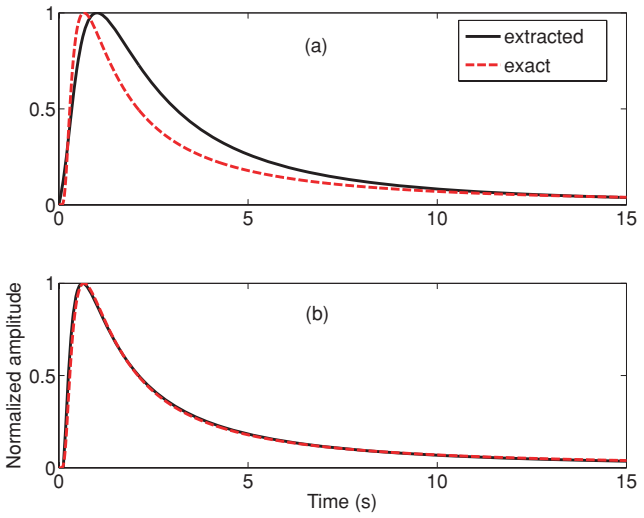

Figure 16. 3-D reconstruction of diffusion Green's function: (a) $W_s = 2.5$ km and $\rho_s = 0.51$ km^{-3}, (b) $W_s = 10$ km and $\rho_s = 0.51$ km^{-3}.

increased, with sufficiently high source density ρ_s, both early and late-time can be extracted well (Fig. 16b).

3 DISCUSSION

3.1 Waves in homogeneous media

The Green's function of the wave equation of a homogeneous medium in 2-D is represented in the frequency domain by the first Hankel function of degree zero (Snieder 2006a)

$$G(r) = \frac{i}{4} H_0^{(1)}(kr). \tag{6}$$

In the numerical simulations for waves in homogeneous media, we use the far-field approximation of eq. (6), which is

$$G(r) = \sqrt{\frac{1}{8\pi kr}}\, e^{i(kr+\pi/4)}. \tag{7}$$

Inserting this into eq. (3), we obtain

$$G(\mathbf{r}_A, \mathbf{r}_B, \omega) - G^*(\mathbf{r}_A, \mathbf{r}_B, \omega) \approx \frac{i}{4\pi\rho} \oint_{S'} \sqrt{\frac{1}{r_{SA} r_{SB}}}\, e^{ik(r_{SA}-r_{SB})} dS', \tag{8}$$

When the source radius is much larger than the distance between the two receivers, the distance in the geometrical spreading can be approximated as $r_{SA} \approx r_{SB} \approx r$, while for the phase the approximation $r_{SA} - r_{SB} \approx b\cos\theta$ is accurate to first order in b/r (These parameters are defined in Fig. 2.) Using these approximations and the relationship $dS' = r\,d\theta$, eq. (8) becomes

$$G(\mathbf{r}_A, \mathbf{r}_B, \omega) - G^*(\mathbf{r}_A, \mathbf{r}_B, \omega) \approx \frac{i}{4\pi\rho} \int_0^{2\pi} e^{ikb\cos\theta} d\theta. \tag{9}$$

Note that the right-hand side does not depend on the source radius r. Experiment 4 in the wave part supports this conclusion: in that experiment, variations in the source radius do not influence the Green's function extraction.

The source radius enters this interferometry problem in three ways. The first is the geometrical spreading term $1/r$, the second is the relationship between the surface element and the increment in source angle $dS' = r\,d\theta$, and the third is the width of the stationary-phase zones as illustrated in the upper panel of Fig. 8. Eq. (9) confirms that the first two factors compensate each other. Consequently, only the width of the stationary-phase zones contribute to the amplitude of the reconstructed signal. The different number of sources in the left- and right-hand stationary-phase zones cause the asymmetry in the amplitude of causal and anticausal response as shown in the lower panel of Fig. 8.

Another interesting observation is that the right-and side of eq. (9) is the integral representation of the Bessel function (Snieder 2006a), which is related to the exact Green's function

$$\frac{1}{2\pi}\int_0^{2\pi} e^{ikb\cos\theta} d\theta = J_0(kb) = \frac{1}{2}\left[H_0^{(1)}(kb) - H_0^{(1)}(-kb)\right]. \tag{10}$$

This shows that by using only far-field of the waves in the interferometry, both far-field and near-field response are reconstructed. This was shown for elastic waves by Sánchez-Sesma *et al.* (2006) and Sánchez-Sesma & Campillo (2006).

For the dependence on the angle θ, we need to study the character of the integrand in eq. (9). The real part of this integrand is the oscillatory function shown in Fig. 17. The extraction of the Green's function depends on the sampling of this integral over source angle θ, and reduces to the numerical integration of a continuous oscillatory function. For a homogeneous source distribution we effectively use Simpson's rule to represent this integral by summation $[\int F(\theta)d\theta \rightarrow \sum_{i=1}^{N} F(\theta_i)\Delta\theta]$. While for random angular distribution, this would not give an accurate estimation with a small number of sources by using summation to replace integral $[\int F(\theta)d\theta \rightarrow \sum_{i=1}^{N} F(\theta_i)\Delta\theta_i]$. If the angle separation for each source is known, we may use $\Delta\theta_i$ as a weight in the summation as it does in the numerical integral. However, if there is no information on $\Delta\theta_i$, the average over repeated experiments with different random distributions converges to a more accurate reconstruction. Fig. 18 shows a histogram of 100 repeated estimations of the integration of the function (Fig. 17) using random sampling points. In each realization, 1000 randomly distributed sources are used to estimate this integral. The estimated value for a specific realization can be far from the exact value while the average over all realizations (dashed line) is close to the accurate value (solid line). For a smoothly varying source angle, $\Delta\theta_i$ is locally fairly constant and

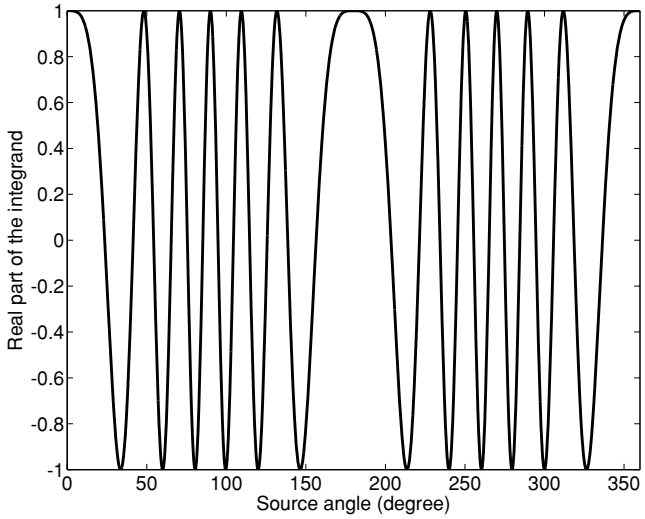

Figure 17. The real part of the integrand in eq. (9).

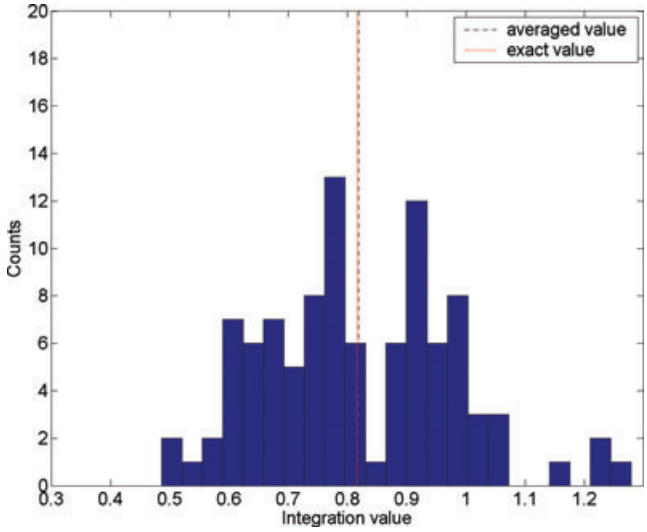

Figure 18. Histogram of 100 repeated estimations of the integral in Fig. 17 using 1000 randomly placed sources in each estimate.

therefore the reconstruction is still accurate with a relatively small number of sources. For most of the applications of interferometry using controlled shots, the source angle is actually smoothly changing (Bakulin & Calvert 2006; Mehta *et al.* 2007). Here we explain why those smooth source angle distributions from experiment 3 for waves give accurate Green's function reconstruction.

What is the minimum required source density if the sources are uniformly distributed in a homogeneous medium? As shown in Fig. 17, the oscillations have a variable period. In order to make the highest frequency oscillations cancel so that the stationary phase contribution remains (Snieder 2004), we need to have enough sampling points at the fastest oscillation. This oscillation depends on the phase term $\Phi = kb\cos\theta$ of eq. (9). The change in the phase for an angular increment $\Delta\theta$ is $\Delta\Phi = kb\sin\theta\Delta\theta$. The most rapid oscillation happens at $\sin\theta = 1$. In order to have N_r number of sources within the period of the most rapid oscillation, the required source density becomes

$$\rho_s = \frac{N_r kb}{2\pi}\ (\text{rad}^{-1}). \tag{11}$$

Based on the numerical simulations, when $N_r > 2.5$, the fluctuation energy between the two main pulses in the reconstruction vanishes, this gives the sampling criterion

$$\rho_s = 0.4kb\ (\text{rad}^{-1}). \tag{12}$$

In practical applications, sources may only be located in the stationary zone. In tat case, there is no need to cancel the high oscillations in Fig. 17, and the required source density can be smaller than the one shown in eq. (12). The source density needed to adequately sample the stationary zone is derived below. The width of the stationary zone (the angle between the two nearest minimum points) is $2\cos^{-1}(1-\pi/kb)$. In order to have N_r number of sources within this stationary zone, the required source density is

$$\rho_s = \frac{N_r}{2\cos^{-1}(1-\pi/kb)}\ (\text{rad}^{-1}). \tag{13}$$

If four sources sample the stationary zone, which in practice is sufficient, the source density is

$$\rho_s = \frac{2}{\cos^{-1}(1-\pi/kb)}\ (\text{rad}^{-1}). \tag{14}$$

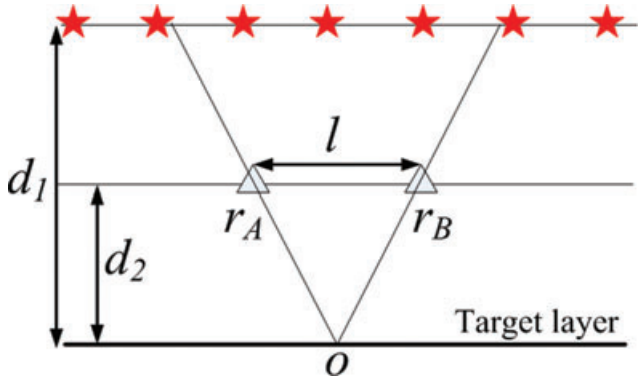

Figure 19. Source and receiver configuration of in an virtual source survey.

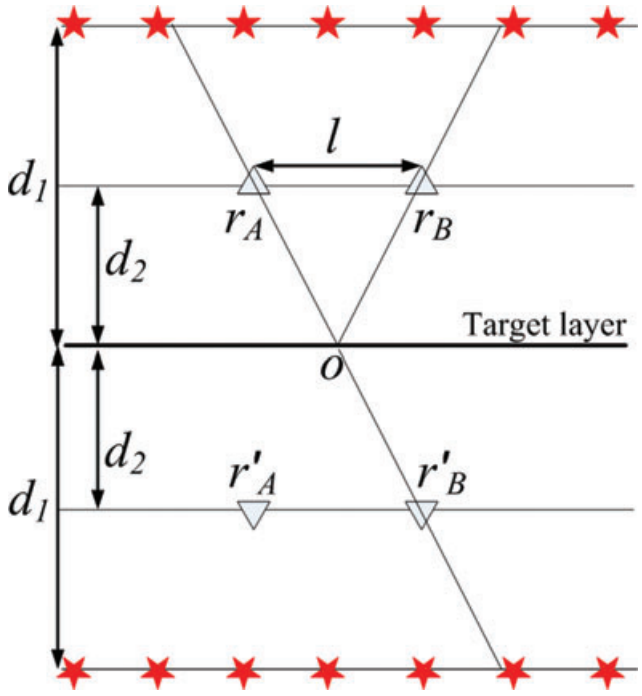

Figure 20. Source and receiver configuration of in an virtual source survey.

Next, we show an application of the derived source density in a virtual source survey. The configuration of the survey is shown in Fig. 19. The sources are denoted by the stars and receivers as triangles. The receivers can be located in an horizontal well in an land survey, or at the ocean bottom in a marine survey. The target layer is at depth d_1 and receivers are at depth $d_1 - d_2$. The two receivers (r_A and r_B) to which interferometry is applied are separated by a distance l. What kind of source distribution is required to apply the interferometry in this configuration? If we use the target layer as a mirror, the configuration in Fig. 19 can be transfer to the one shown in Fig. 20. Term b in eqs (11) and (13) becomes $\sqrt{4d_2^2 + l^2}$. Source radius r (distance from reflection point O to sources in the stationary phase zone) is $\sqrt{d_2^2 + l^2/4}d_1/d_2$. Apply these parameters to eq. (12) and the source density on the surface becomes

$$\mathrm{d}r = r\rho_s = \frac{0.8k\left(d_2^2 + l^2/4\right)d_1}{d_2}\ (\text{m}^{-1}). \tag{15}$$

This is the required source density if the contributions from the fastest oscillations in Fig. 17 must cancel. If only the sources in the

stationary zone are used in the summation, eq. (14) should be used and source density on the surface becomes

$$\mathrm{d}r = \frac{d_1\sqrt{4d_2^2 + l^2}}{d_2 \cos^{-1}\left[1 - \pi/\left(k\sqrt{4d_2^2 + l^2}\right)\right]}\ (\mathrm{m}^{-1}). \tag{16}$$

In conclusion, for wave interferometry in a homogeneous model, the most important parameter is the source angle distribution. If we know the source distribution, and hence the source angle, different weighting of the sources can be used to more accurately replace the integral over sources by a sum over sources. If randomly distributed sources are used and there is no information on the source angle distribution, the average of a large amount of extracted signals is more accurate to describe the real response than a single extracted signal.

This conclusion holds when all sources have the same amplitude. If the amplitude of the sources fluctuates randomly, a uniform angle distribution gives similar reconstruction of the Green's function as the random angle distribution for a constant source strength.

3.2 Waves in heterogeneous media

We find that one single source never gives an accurate Green's function reconstruction in the open scattering medium used in the example (see Fig. 11). In contrast, a dense source distribution is still needed in this strongly scattering medium. In our numerical experiment 140 uniformly distributed sources are enough to reconstruct the Green's function accurately if the scatterers are absent (homogeneous medium). This number is consistent with the criterion of expression (12). This suggests that more sources are needed to reconstruct the full Green's function accurately for this heterogeneous medium (300 sources) than the homogeneous medium with the same parameters (140 sources). This contradicts the common notion that the heterogeneity around the receivers would reduce the required number of sources. When the wave propagation is equipatitioned in the heterogeneous medium (propagation path $\gg$ transport mean free path l_*), the wave field is diffusive. Cross-correlating these diffusive fields at two receiver locations is believed to give the Green's function between two locations (Lobkis & Weaver 2001). Because of the equipatitioning one might think that the source distribution should not matter. This is not what we observe in our numerical experiment (Fig. 11), as 200 isotropic scatters in our experiment suffice to produce equipatitioning.

The optical theorem states that the total scattering cross section in 2-D medium can be represented as $\sigma = -\mathrm{Im}A/k_0$ (Groenenboom & Snieder 1995), in which $\mathrm{Im}A$ is the imaginary component of the forward scattering amplitude A and k_0 is the wave vector in the background medium. For isotropic scatters, the imaginary component of A is restricted by $-4 \leq \mathrm{Im}A \leq 0$ because of the energy conservation (Groenenboom & Snieder 1995). In our numerical experiment, $\mathrm{Im}A$ is chosen to be -3.99 to give strong scattering. For isotropic scatterers, the transport mean free path l_* is equal to the scattering mean free path (Ishimaru 1997). The scattering mean free path is given by $l_s = 1/(N\sigma)$, in which N is the density of scatterers (Sheng 1990). Using these expressions, the transport mean free path in our 200 isotropic scatterers area is about 5 m and the transport mean free time is about 3 ms. As the shortest propagation path in the heterogeneous area from a source to a receiver is 30 m, the earliest signal arrives at the receivers has propagated 6 mean free path in the heterogeneous area; therefore the energy flow associated with wave propagation is very close to being equipatitioned. We also cross correlated the later part of the signal (later than 50 mean free times) but the cross-correlation does not give the full Green's function at all with the 300 random sources. This raises a fundamental question: is equipationing a necessary condition in Green's function reconstruction, or is it a sufficient condition? Our experiment suggests that equipatitioning is necessary but not sufficient. A source distribution with a sufficiently large aperture and source density is still important to retrieve the full Green's function.

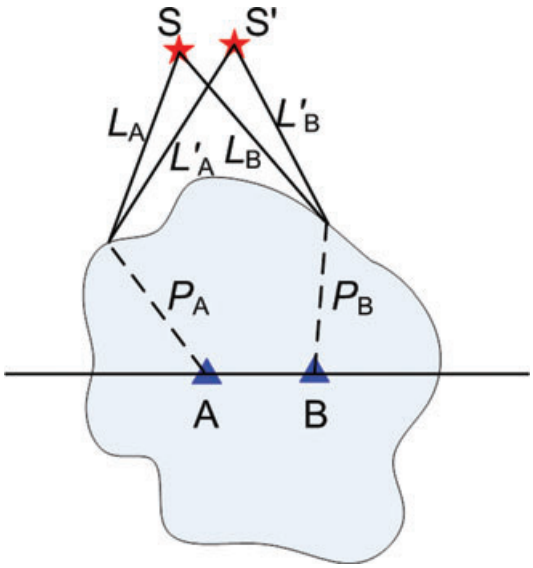

Figure 21. The configuration of wave propagation with receivers in a heterogeneous area.

Another question is how we can understand that more sources are needed in this heterogeneous medium than that in the homogeneous one? To answer this question, we show in Fig. 21 a medium with heterogeneity (scatterers) around the receivers. The stars are sources and triangles are receivers. The gray part represents the heterogeneous area. The signal recorded at each receiver is the superposition of wavefields from all possible scattering paths. First, consider one possible path of wave propagation from source S to receiver A. The wave hits the first scatterer (not necessary to be a scatterer on the boundary of the heterogeneous area) after a propagation distance L_A and then propagates to receiver A in the heterogeneous part in a complicated path with a propagation distance P_A. The dashed lines in Fig. 21 means that we do not know the exact path from the first scatterer to the receivers. Another possible path from source S to receiver B is also shown in the same manner. When we cross-correlate these two fields received at A and B from source S, the phase of the cross-correlation is $\phi = k(L_\mathrm{A} - L_\mathrm{B}) + (\phi_\mathrm{A} - \phi_\mathrm{B})$, in which k is the wave numbers in the homogeneous area, ϕ_A and ϕ_B are the phase shifts along the paths P_A and P_B, respectively. When the source is moved with a small step from S to S′, the propagation paths in the heterogeneous area P_A and P_B stay the same while the paths in the homogeneous part changed to L'_A and L'_B. The phase of the cross-correlation becomes $\phi' = k(L'_\mathrm{A} - L'_\mathrm{B}) + (\phi_\mathrm{A} - \phi_\mathrm{B})$. Therefore, the phase change of the cross-correlation when the source is moved from S to S′ is $\Delta\phi = k(L'_\mathrm{A} - L_\mathrm{A}) - k(L'_\mathrm{B} - L_\mathrm{B})$. We can quantify this phase change using the parameters shown in Fig. 22. The angle between the path from the source to the first scatterers and the source radius r is defined as α. From the geometry of Fig. 22, we obtain $L'_\mathrm{A} - L_\mathrm{A} = \mathrm{d}r \sin\alpha_\mathrm{A}$. Similarly we can get $L'_\mathrm{B} - L_\mathrm{B} = -\mathrm{d}r \sin\alpha_\mathrm{B}$. Therefore, the phase change is given by

$$\Delta\phi = k(\sin\alpha_\mathrm{A} + \sin\alpha_\mathrm{B})\mathrm{d}r. \tag{17}$$

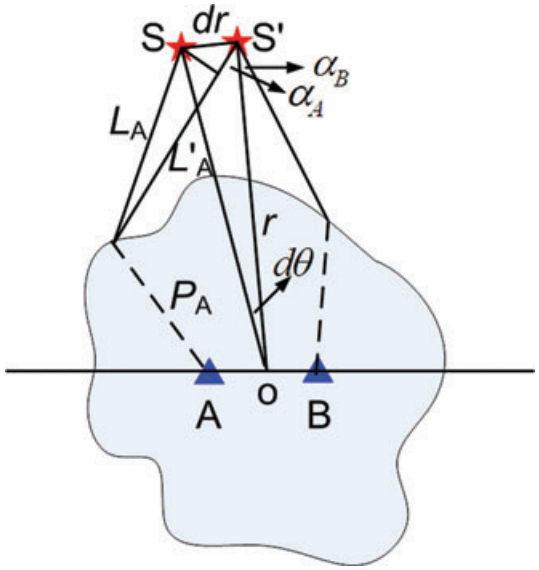

Figure 22. Parameters used to quantify the phase change in cross-correlation

In order to avoid aliasing, this phase change should be smaller than $\pi/2$. Consequently, we obtain the following criterion for the source separation

$$dr \leq \frac{\pi}{2k(\sin\alpha_A + \sin\alpha_B)}. \tag{18}$$

Applying $k = 2\pi/\lambda$, the criterion becomes

$$dr \leq \frac{\lambda}{\sin\alpha_A + \sin\alpha_B}. \tag{19}$$

Eq. (19) shows that the source density is controlled by the size and position of the heterogeneous area with respect to the source position, rather than by the heterogeneity itself. When heterogeneity appears around the receivers, the maximum angle between the source radius and the path from the source to the first scatterer becomes larger. In eq. (19), it means $\alpha_{A,B}$ increases. Consequently, the required source separation dr needs to be smaller than that for homogeneous medium. Therefore, more sources are needed for the heterogeneous medium than for the homogeneous one.

If one is interested in the direct arrival Green's function only, the requirement of the source distribution can be relaxed. For example, Malcolm *et al.* (2004) showed that the ensemble-averaged Green's function in a granite can be retrieved from a single source by averaging over a pair of receivers with constant offset. The low frequency component of the direct surface wave Green's function has been retrieved from several irregularly distributed earthquakes (Campillo & Paul 2003). However, the full Green's function is not retrieved in those studies. One interesting study shows that in a layered model with enough horizontal layers to give strong scattering and refraction, the full Green's function can be reconstructed by one-sided illumination with sources uniformly distributed on the free surface (Wapenaar 2006a). In his 1-D layered model with normal-incident plane wave, the subsurface acts like a mirror when the heterogeneity of the layers is strong enough, with the result that sources on one side suffice for the Green's function reconstruction.

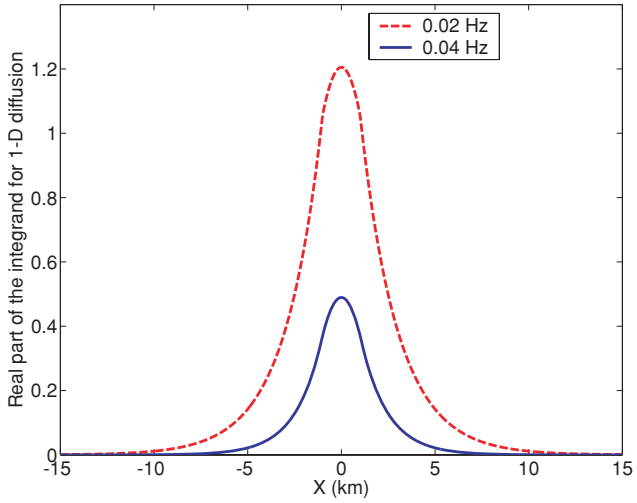

Figure 23. The real part of the integrand in eq. (21) at two different frequencies.

3.3 Diffusion

The frequency domain Green's function of the diffusion equation in a 1-D homogeneous medium is given by

$$G^{1D}(x,\omega) = \frac{1}{(1+i)\sqrt{2\omega D}} e^{(-1-i)x\sqrt{\omega/2D}}. \tag{20}$$

Inserting this expression into eq. (4), gives

$$G(\mathbf{r}_A,\mathbf{r}_B,\omega) - G^*(\mathbf{r}_A,\mathbf{r}_B,\omega) = \frac{i}{2D}\int_x e^{-(r_{SA}+r_{SB})\sqrt{\omega/2D}} e^{-i(r_{SA}-r_{SB})\sqrt{\omega/2D}} dx, \tag{21}$$

in which r_{SA} and r_{SB} are the distances between the source to the receiver A and B, respectively. Similar as for the analysis of the waves, we study the real part of the integrand of eq. (21) as a function of source position x. Notice that the integrand is a function of frequency ω. Fig. 23 shows the real part of this integrand for two different frequencies. The width of the distribution decreases with frequency. Qualitatively we can conclude that because the early-time behaviour of the Green's function has more high-frequency components, the required source distribution can be narrower. This explains experiment 1 of the diffusion part: with small W_s, the early-time behaviour is reconstructed well. With increasing W_s, more lower frequency components are recovered. Since the tail of the Green's function mostly contains low frequencies, the late-time Green's function is recovered accurately with a large width W_s. Consequently, the source density ρ_s controls the retrieval of the high-frequency components of the Green's function (eg. early-time of the Green's function), and the width of the distribution W_s controls lower frequency components (e.g. the late-time of the Green's function).

The frequency domain Green's function for diffusion in 3-D is

$$G^{3D}(r,\omega) = \frac{1}{4\pi Dr} e^{(-1-i)r\sqrt{\omega/2D}}. \tag{22}$$

Inserting this into eq. (4) we obtain

$$G(\mathbf{r}_A,\mathbf{r}_B,\omega) - G^*(\mathbf{r}_A,\mathbf{r}_B,\omega) = 2i\omega\int_V \frac{1}{(4\pi D)^2 r_{SA} r_{SB}} e^{-(r_{SA}+r_{SB})\sqrt{\omega/2D}} e^{-i(r_{SA}-r_{SB})\sqrt{\omega/2D}} dV. \tag{23}$$

The integrand of eq. (23) has two singularities at the receiver positions where r_{SA} and r_{SB} vanish. The integrand in eq. (23) is largest

for the sources near the receivers. In fact, it has an integrable singularity. One needs to integrate over this singularity to retrieve the exact Green's function since the integrand of eq. (23) itself is not equal to the Green's function.

We next address the question how to quantify the required source distribution width W_s and source density ρ_s. As we learned from the examples in the diffusion part, W_s determines the late-time reconstruction of the Green's function. We define τ_a to be the time up to which we want to reconstruct the Green's function accurately. Sources within a source–receiver distance $r^2_{\max}/(4D\tau_a) = 1$ give the largest contribution (Mehrer 2007). Therefore, the required W_s should be

$$W_s = 4\sqrt{D\tau_a} + b \tag{24}$$

for an accurate reconstruction up to time τ_a, in which b is the distance between the two receivers. We define the error as the ratio of the difference between the exact and extracted signals to the exact signal at time τ_a. The error is less than 5 per cent with W_s from the criterion 24.

The source density ρ_s controls the early-time reconstruction. In other words, it determines the accuracy of the reconstruction for the high-frequency components. For the maximum frequency f_m in the problem—either the highest frequency component of the Green's function itself or the maximum frequency of the source function—there is a sensitivity function of source position. This sensitivity is controlled by the decay factor $e^{-(r_{SA}+r_{SB})\sqrt{\omega/2D}}$ as shown in eqs (21) and (23). The $1/e$ width of this sensitivity function is

$$\sigma = \sqrt{2D/\omega}. \tag{25}$$

Then if N_r is the number of sources needed in this range σ to estimate the integral accurately, the required source density is

$$\rho_{SA} = N_r\sqrt{\omega/2D}. \tag{26}$$

Based on the numerical examples, when N_r is larger than 2, the early-time response is reconstructed accurately. Then criterion (26) becomes

$$\rho_{SA} = 2\sqrt{\omega/2D}. \tag{27}$$

We can estimate the maximum frequency component in the Green's function as $1/(4t_p)$, in which t_p is the arrival time of the amplitude peak in the Green's function. We define the error as the ratio of the difference between the exact and extracted signals to the exact signal at time $t_p/2$. The error is less than 5 per cent with source density from the criterion in eq. (27).

In conclusion, for cross-correlation-based diffusion interferometry, instead of having sources everywhere in the volume, it suffices to have sources in only a small volume surrounding the receivers. For the 1-D problem, the source distribution width controls the late-time (low-frequency components) reconstruction of the Green's function and source density controls the early-time (high-frequency components) reconstruction. For the 3-D problem, sources should not be located too close to the receivers position because of the singularities at those points.

4 CONCLUSION

Cross-correlation-based interferometry used to extract the Green's function which describes the field propagation between two receivers can be applied to the solution of both the wave equation and the diffusion equation. The main difference is the required source distribution.

For wave interferometry in a homogeneous medium, the source angle distribution is the most important parameter. With the assumption that the source radii are much larger than the distance between the two receivers, the variation in the source radius has a negligible effect, and the interferometry problem can be represented by a numerical integral of an oscillatory function of source angle. If cross-correlations from different sources are simply added in the Green's function extraction, the uniform source angle distribution gives a high decay rate of the non-physical fluctuation as a function of number of sources (faster than N^{-10}). With the same number of sources, the random distribution gives much poorer Green's function reconstruction. The rate of the non-physical fluctuation decay is approximately N^{-1}. The decay rate of the smoothly angular varying distribution is between those of uniform and random distributions and depends on how smooth the source angle varies. The required source density is determined by the distance between the two receivers and the wavenumber.

For wave interferometry in a heterogeneous medium, one single source is not sufficient to give accurate reconstruction even the wavefield is equipartitioned. This suggests that equipartition is a necessary but not sufficient condition in the Green's function reconstruction. Besides, more sources are needed to reconstruct the full Green's function in an heterogeneous medium than that for an homogeneous medium. The required source density is determined by the position and size of the heterogeneous area with respect to the sources.

For diffusion interferometry in a homogeneous medium, although the study shows that a finite number of sources suffice to reconstruct the Green's function, the cross-correlation-based interferometry is not applicable for real applications because the sources are required to be close to the receivers. For a 1-D model, the sensitivity of the sources decays from the centre of the two receivers. The width of the distribution controls the late-time of the reconstructed Green's function while the source density controls the early-time of the reconstructed Green's function. For a 3-D model, the main properties are the same as for the 1-D problem. The important point is that the sources between the two receivers give most of the contribution and these source distributions are hard to realize in practice. Because the requirement on the source distribution for diffusion interferometry is difficult to match in practice, it is preferable to use multidimensional deconvolution methods instead of correlation for diffusive fields, such as low-frequency electromagnetic fields (Wapenaar *et al.* 2008; Snieder *et al.* 2009).

ACKNOWLEDGMENTS

This work is supported by the Shell GameChanger project. We appreciate the valuable discussions and suggestions from our colleagues in the Center for Wave Phenomena and Kees Wapenaar, Evert Slob from Delft University of Technology, Netherlands.

REFERENCES

Bakulin, A. & Calvert, R., 2004. Virtual source: new method for imaging and 4D below complex overburden, *SEG Tech. Prog. Expand. Abst.,* **23,** 2477–2480.

Bakulin, A. & Calvert, R., 2006. The virtual source method: theory and case study, *Geophysics,* **71,** SI139–SI150.

Bourdet, D., 2002. *Well Test Analysis (Handbook of Petroleum Exploration and Production)*, 1st edn, Elsevier Science, Amsterdam.

Calvert, R., Bakulin, A. & Joners, T.C., 2004. Virtual sources, a new way to remove overburden problems, in *Expanded Abstracts of the 2004 EAEG-Meeting*, pp. 2477–2480.

Campillo, M. & Paul, A., 2003. Long-range correlations in the diffuse seismic coda, *Science,* **299,** 547–549.

Constable, S. & Srnka, L.J., 2007. An introduction to marine controlled-source electromagnetic methods for hydrocarbon exporation, *Geophysics,* **72,** WA3–WA12.

Curtis, A., Gerstoft, P., Sato, H., Snieder, R. & Wapenaar, K., 2006. Seismic interferometry-turning noise into signal, *Leading Edge,* **25,** 1082–1092.

Darnet, M., Choo, M.C.K., Plessix, R.E., rosenquist, M.L., Yip-Cheong, K., Sims, E. & Voon, J.W.K., 2007. Detecting hydrocarbon reservoirs from CSEM data in complex setting: application to deepwater Sabah, Malaysia, *Geophysics,* **72,** WA97–WA103.

Derode, A., Larose, E., Campillo, M. & Fink, M., 2003. How to estimate the Green's function of a heterogeneous medium between two passive sensors? Application to acoustic waves, *Appl. Phys. Lett.,* **83,** 3054–3056.

Godin, O.A., 2006. Recovering the acoustic Green's function from ambient noise cross correlation in an inhomogeneous moving medium, *Phys. Rev. Lett.,* **97,** 054301–4.

Groenenboom, J. & Snieder, R., 1995. Attenuation, dispersion and anisotropy by multiple scattering of transmitted waves through distributions of scatterers, *J. acoust. Soc. Am.,* **98,** 3482–3492.

Hoversten, G.M., Newman, G.A., Geier, N. & Flanagan, G., 2006. 3D modeling of a deepwater EM exploration survey, *Geophysics,* **71,** G239–G248.

Ishimaru, A., 1997. *Wave Propagation and Scattering in Random Media*, IEEE Press, Piscataway, NJ and Oxford University Press, NY.

Kutasov, I.M., Eppelbaum, L.V. & Kagan, M., 2008. Interference well testing—variable fluid flow rate, *J. Geophys. Eng.,* **5,** 86–91.

Larose, E., Montaldo, G., Derode, A. & Campillo, M., 2006. Passive imaging of localized reflectors and interfaces in open media, *Appl. Phys. Lett.,* **88,** 104103, doi:10.1063/1.2186112.

Lobkis, O.I. & Weaver, R.L., 2001. On the emergence of the Green's function in the correlations of a diffuse field, *J. acoust. Soc. Am.,* **110,** 3011–3017.

Malcolm, A.E., Scales, J.A. & van Tiggelen, B.A., 2004. Extracting the Green function from diffuse, equipartitioned waves, *Phys. Rev. E.,* **70,** 015601, doi:10.1103/PhysRevE.70.015601.

Mehrer, H., 2007. *Diffusion in Solids—Fundamentals, Methods, Materials, Diffusion-Controlled Processes*, Springer, Berlin Heidelberg, New York.

Mehta, K. & Snieder, R., 2008. Acquisition geometry requirements for generating virtual-source data, *Leading Edge,* **27,** 620–629.

Mehta, K., Bakulin, A., Sheiman, J., Calvert, R. & Snieder, R., 2007. Improving the virtual source method by wavefield separation, *Geophysics,* **72,** V79–V86.

Miyazawa, M., Snieder, R. & Venkataraman, A., 2008. Application of seismic interferometry to extract P and S wave propagation and observation of shear wave splitting from noise data at cold lake, canada, *Geophysics,* **73,** D35–D40.

Rickett, J. & Claerbout, J., 1999. Acoustic daylight imaging via spectral factorization: Helioseismology and reservoir monitoring, *Leading Edge*, pp. 957–960.

Roux, P., Sabra, K.G., Kuperman, W.A. & Roux, A., 2005. Ambient noise cross correlation in free space: theoretical approach, *J. acoust. Soc. Am.,* **117,** 79–84.

Sabra, K.G., Gerstoft, P., Roux, P., Kuperman, W.A. & Fehler, M.C., 2005a. Extracting time-domain Green's function estimates from ambient seismic noise, *Geophys. Res. Lett.,* **32,** L03310, doi:10.1029/2004GL021862.

Sabra, K.G., Gerstoft, P., Roux, P., Kuperman, W.A. & Fehler, M.C., 2005b. Surface wave tomography from microseisms in southern California, *Geophys. Res. Lett.,* **32,** L14311, doi:10.1029/2005GL023155.

Sánchez-Sesma, F. & Campillo, M., 2006. Retrieval of the Green's funciton from cross correlation: the canonical elastic problem, *Bull. seism. Soc. Am.,* **96,** 1182–1191.

Sánchez-Sesma, F., Pérez-Ruiz, J., Campillo, M. & Luzón, F., 2006. Elastodynamic 2D Green function retrieval from cross-correlation: canonical inclusion problem, *Geophys. Res. Lett.,* **33,** L13305, doi:10.1029/2006GL026454.

Scholl, C. & Edwards, R.N., 2007. Marine downhole to seafloor dipole-dipole electromagnetic methods and the resolution of resistive targets, *Geophysics,* **72,** WA39–WA49.

Schuster, G.T., Yu, J., Sheng, J. & Rickett, J., 2004. Interferometric/daylight seismic imaging, *Geophys. J. Int.,* **157,** 838–852.

Shapiro, N.M., Campillo, M., Stehly, L. & Ritzwoller, M.H., 2005. High-resolution surface-wave tomography from ambient seismic noise, *Science,* **307,** 1615–1618.

Sheng, P., 1990. *Scattering and Localization of Classical Waves in Random Media*, World Scientific, Singapore.

Snieder, R., 2004. Extracting the Green's function from the correlation of coda waves: A derivation based on stationary phase, *Phys. Rev. E,* **69,** 046610, doi:10.1103/PhysRevE.69.046610.

Snieder, R., 2006a. *A Guided Tour of Mathematical Methods For the Physical Sciences*, 2nd edn, Cambridge University Press, Cambridge.

Snieder, R., 2006b. Retrieving the Green's function of the diffusion equation from the response to a random forcing, *Phys. Rev. E,* **74,** 046620, doi:10.1103/PhysRevE.74.046620.

Snieder, R., 2007. Extracting the Green's function of attenuating heterogeneous acoustic media from uncorrelated waves, *J. acoust. Soc. Am.,* **121,** 2537–2643.

Snieder, R. & Şafak, E., 2006. Extracting the building response using seismic interferometry: Theory and application to the Millikan library in Pasadena, California, *Bull. seism. Soc. Am.,* **96,** 586–598.

Snieder, R., Sheiman, J. & Calvert, R., 2006. Equivalence of the virtual-source method and wave-field deconvolution in seismic interferometry, *Phys. Rev. E,* **73,** 066620, doi:10.1103/PhysRevE.73.066620.

Snieder, R., Wapenaar, K. & Wegler, U., 2007. Unified Green's function retrieval by cross-correlation: connection with energy principles, *Phys. Rev. E.,* **75,** 036103, doi:10.1103/PhysRevE.75.036103.

Snieder, R., Miyazawa, M., Slob, E., Vasconcelos, I. & Wapenaar, K., 2009. A comparison of strategies for seismic interferometry, *Surv. Geophys.,* **30,** 503–523.

Stehly, L., Campillo, M. & Shapiro, N.M., 2006. A study of seismic noise from its long-range correlation properties, *J. Geophys. Res.,* **111,** B10306, doi:10.1029/2005JB004237.

van Manen, D., Robertsson, J.O.A. & Curtis, A., 2005. Modeling of wave propagation in inhomogeneous media, *Phys. Rev. Lett.,* **94,** 164301, doi:10.1103/PhysRevLett.94.164301.

van Wijk, K., 2006. On estimating the impulse response between receivers in a controlled ultrasonic experiment, *Geophysics,* **71,** SI79–SI84.

Vasconcelos, I. & Snieder, R., 2008a. Interferometry by deconvolution. Part 1—theory for acoustic waves and numerical examples, *Geophysics,* **73,** S115–S128.

Vasconcelos, I. & Snieder, R., 2008b. Interferometry by deconvolution. Part 2—elastic waves and application to drill-bit seismic imaging, *Geophysics,* **73,** S129–S141.

Vasconcelos, I., Snieder, R. & Hornby, B., 2007. Target-oriented interferometry—imaging with internal multiples from subsalt VSP data, *SEG Tech. Prog. Expand. Abst.,* **26,** 3069–3073.

Wapenaar, K., 2004. Retrieving the elastodynamic Green's function of an arbitrary inhomogeneous medium by cross correlation, *Phys. Rev. Lett.,* **93,** 254301, doi:10.1103/PhysRevLett.93.254301.

Wapenaar, K., 2006a. Green's function retrieval by cross-correlation in case of one-sided illumination, *Geophys. Res. Lett.,* **33,** L19304, doi:10.1029/2006GL027747.

Wapenaar, K., 2006b. Non-reciprocal Green's function retrieval by cross correlation, *J. Acoust. Soc. Am.,* **120,** EL7–EL13.

Wapenaar, K., Fokkema, J. & Snieder, R., 2005. Retrieving the Green's function in an open system by cross-correlation: a comparison of approaches, *J. acoust. Soc. Am.,* **118,** 2783–2786.

Wapenaar, K., Slob, E. & Snieder, R., 2006. Unified Green's function retrieval by cross correlation, *Phys. Rev. Lett.,* **97,** 234301, doi:10.1103/PhysRevLett.97.234301.

Wapenaar, K., Slob, E. & Snieder, R., 2008. Seismic and electromagnetic controlled-source interferometry in dissipative media, *Geophys. Prospect.,* **56,** 419–434.

Weaver, R., 2008. Ward identities and the retrieval of Green's functions in the correlations of a diffuse field, *Wave Motion,* **45,** 596–604.

Weaver, R.L., 2005. Information from seismic noise, *Science,* **307,** 1568–1569.

Weaver, R.L. & Lobkis, O.I., 2001. Ultrasonics without a source: thermal fluctuation correlations at MHz frequencies, *Phys. Rev. Lett.,* **87,** 134301, doi:10.1103/PhysRevLett.87.134301.

Weaver, R.L. & Lobkis, O.I., 2004. Diffuse fields in open systems and the emergence of the Green's function., *J. acoust. Soc. Am.,* **116,** 2731–2734.

Weaver, R.L. & Lobkis, O.I., 2005. Fluctuations in diffuse field–field correlations and the emergence of the Green's function in open systems, *J. acoust. Soc. Am.,* **117,** 3432–3439.